Interannual Variability and Annual Cycle: Mechanisms of Circulation and Climate in the Tropical Atlantic Sector

STEFAN HASTENRATH

Department of Meteorology, The University of Wisconsin, Madison, WI 53706

(Manuscript received 27 May 1983, in final form 29 February 1984)

ABSTRACT

General circulation mechanisms instrumental in both annual cycle and interannual variability of rainfall are studied with reference to key regions of the tropical Americas and Africa, including the Central American–Caribbean area, northern Northeast Brazil, Subsaharan Africa, the Angola coast and the Zaïre (Congo) and Amazon basins. For most of these regions, rainfall anomalies tend to be associated with departures in the large-scale atmospheric and oceanic fields that correspond to the pattern changes in the annual alternation of dry and rainy seasons. The interannual variability of climate and circulation thus appears largely as enhancement and reduction of the annual cycle.

1. Introduction

In the study of climate, the annual cycle is widely regarded as one of the more elementary topics. For the tropical Atlantic domain, much of the basic facts regarding climate are indeed well documented by surface and upper-air atlases (Jackson, 1964; Thompson, 1965; Taljaard *et al.*, 1969; Sadler, 1975; Hastenrath and Lamb, 1977a, 1978a; Chu and Hastenrath, 1982). Supported by such background climatology, investigations were undertaken in the past decade into the interannual variability of climate and its general circulation causes. A series of circum-Atlantic studies (Hastenrath, 1976, 1978; Hastenrath and Heller, 1977; Hastenrath and Lamb, 1977b, 1978b; Markham and McLain, 1977; Lamb, 1978a,b, 1984; Covey and Hastenrath, 1978; Moura and Shukla, 1981; Chu, 1983; Hirst and Hastenrath, 1983a,b) has gradually elucidated the general circulation mechanisms instrumental in the development of hydrometeorological extreme events in various key regions. In the course of this work it became increasingly apparent that the mechanisms of interannual variability of circulation and climate are in large part related to the functioning of the annual cycle, which itself is not well understood. The present paper uses our series of circum-Atlantic studies to reexamine the general circulation mechanisms of regional climate anomalies in the tropical Atlantic sector and, in particular, to assess these anomalies in perspective with the operation of the annual cycle.

2. Observations

Ship observations over the tropical Atlantic between 30°N and 30°S during the period 1911–72 obtained from the National Climatic Center at Asheville, North Carolina, have been processed by one degree square areas (Hastenrath and Lamb, 1977a; Hastenrath and Heller, 1977), and subsequently compiled into 5 degree square values. Elements of interest here include sea level pressure (SLP), surface zonal (u) and meridional (v) components of wind, sea surface temperature (SST) and total cloudiness. The density of ship observations is illustrated in Hastenrath and Lamb (1977a) and in Fig. 1.

Upper-air observations in the tropical Americas and Africa since the late 1950s are published in U.S. Weather Bureau, ESSA, NOAA (1958-81). Records of selected surface stations are contained in the latter publication and in publications of the Smithsonian Institution (1927, 1934, 1947), U.S. Weather Bureau (1959) and Environmental Sciences Service Administration, ESSA (1967). Based on a variety of unpublished rainfall, river and lake level observations and the aforementioned sources, hydrometeorological index series representative of key tropical land areas were compiled in our various earlier circum-Atlantic studies (Hastenrath, 1976, 1978; Hastenrath and Heller, 1977; Covey and Hastenrath, 1978; Lamb, 1978a,b; Hirst and Hastenrath, 1983a,b; Chu, 1983). The present paper draws on this data bank.

3. The annual cycle

The purpose of this section is to sketch the annual march of the general circulation in the tropical Atlantic sector and to summarize the seasonality of rainfall in key land areas for which the mechanisms of interannual variability have been comprehensively studied.

The annual cycle characteristics of the surface circulation are documented in detail by monthly charts

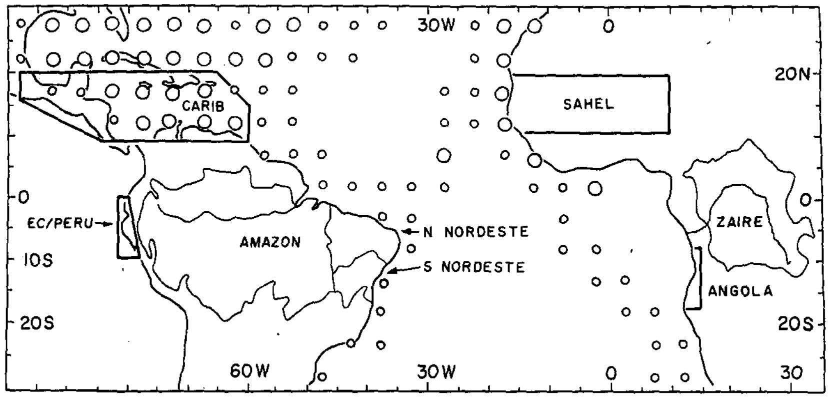

FIG. 1. Orientation map. Key tropical land areas are: Central American–Caribbean region (CARIB), Ecuador–Peru coast (EC/PERU), northern and southern Northeast Brazil (N NORDESTE, S NORDESTE), Amazonia (AMAZON), Subsaharan Africa (SAHEL), Zaïre (Congo) basin (ZAIRE), Angola coast (ANGOLA). Large and small open circles indicate, respectively, five degree squares with >50 000 and 10 000–50 000 ship observations during 1911–72.

in Hastenrath and Lamb (1977a). On the whole, the extrema of the annual cycle are reached around the end of August and February. Thus, the most salient features of the annual march of atmospheric and hydrospheric fields can be illustrated by August–September minus February–March difference charts, as presented here for SLP (Fig. 2a), u and v components of surface wind (Figs. 2b, c) SST (Fig. 2d), divergence (Fig. 2e) and total cloudiness (Fig. 2f). While it is uncommon to describe the annual variation of large-scale atmospheric and hydrospheric fields by difference maps, these provide a suitable reference for comparing the annual cycle and interannual variability (Section 4).

Thus, Fig. 2a shows large negative SLP differences in most of the North Atlantic north of ~10°N, and positive values over the equatorial and South Atlantic, reflecting the seasonal shifts of the subtropical highs and the enclosed near-equatorial trough of low pressure. In Fig. 2b, the intra-annual changes in the position and intensity of circulation belts are reflected in the large positive difference of the westerly wind component—signifying weaker easterlies during northern summer—in a broad band between the equator and ~20°N, extending from the African coast to the Americas, and the differences of opposite sign over the equatorial South Atlantic. Similarly, Fig. 2c shows large positive differences of the southerly wind component in the equatorial zone of both hemispheres, which corresponds to the enhanced cross-equatorial flow emanating from the South Atlantic high during northern summer. Fig. 2d is dominated by positive SST differences in the North Atlantic and negative values in the South Atlantic, thus reflecting the seasonal thermal contrasts between hemispheres. Aside from these hemispheric-scale SST characteristics, the following features stand out: a band of large positive differences at about 10–20°N extending from the West African coast all across the Atlantic to the Americas; negative values in a tongue immediately to the south of the eastern and central Atlantic equator, that is, in the region of cold water upwelling during the northern summer (Hastenrath and Lamb, 1977a,b); and large negative values in the eastern South Atlantic off the coast of Southwest Africa. Most prominent in Fig. 2e is the bandlike arrangement of differences in divergence, broadly reflecting the northward displacement of the near-equatorial convergence band during northern summer (Hastenrath and Lamb, 1977a); this is further illustrated in Fig. 6. The cloudiness differences in Fig. 2f show a similar zonal arrangement. Figs. 2a–f thus repeat the information content of our atlas (Hastenrath and Lamb, 1977a) in a form more suitable for the discussion of interannual variability.

The annual march of atmospheric events in the tropics is primarily reflected in the rainfall activity. The general circulation causes of the alternation of rainy and dry seasons in the various land areas are reviewed in the following.

The Central American–Caribbean region (CARIB in Fig. 1) experiences its rainy season during the northern summer half-year, when the North Atlantic high is displaced northward, the downstream portion of the trades convergent, the trade inversion high and weak (Hastenrath, 1966, 1967, 1976), the ocean warm and atmospheric moisture abundant. By contrast, February–March is the driest time of the year in most of the area, coincident with a tendency of lower-tropospheric divergence and subsidence, strong trade inversion, cold ocean and reduced atmospheric humidity.

The rainfall in northern Northeast Brazil (N NORDESTE in Fig. 1) is narrowly concentrated in March–April (Hastenrath and Heller, 1977). The following general circulation factors favor the rainfall ac-

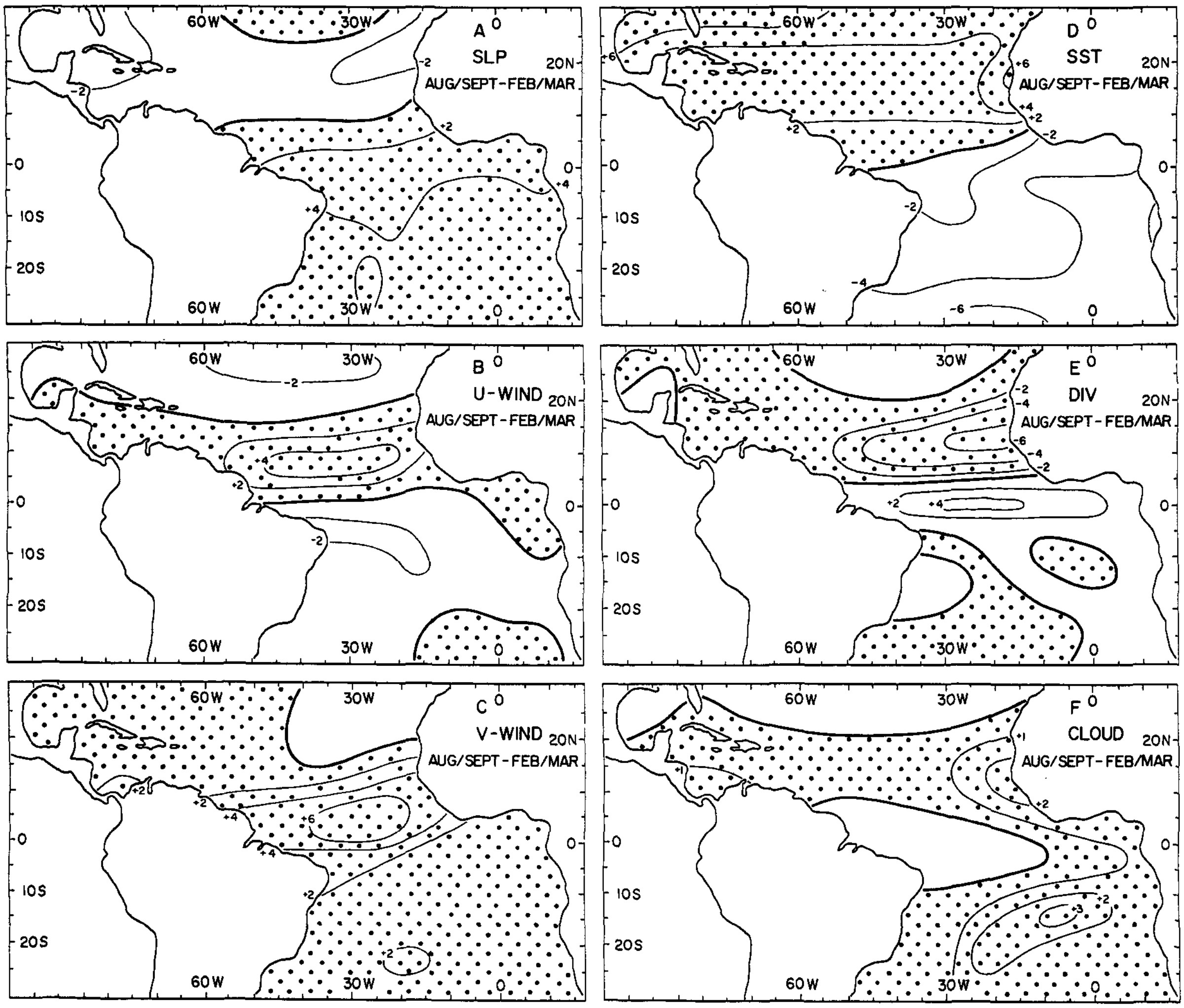

FIG. 2. Maps of 1911–70 average August–September minus February–March difference of (a) SLP in mb; (b) zonal u and (c) meridional v components of wind in m s^{-1}; (d) SST in °C; (3) divergence in 10^{-6} s^{-1}; (f) total cloudiness in tenths. Dot raster denotes positive areas, except for chart (e) where it indicates convergence.

tivity at this time of year: 1) the convergence band over the Atlantic reaches its southernmost, always Northern Hemispheric location; 2) the equatorial South Atlantic is comparatively warm and the North Atlantic cold, so that a thermally direct meridional circulation cell in the atmosphere (Moura and Shukla, 1981) would entail decreased subsidence and enhanced ascending motion over Northeast Brazil and the adjacent equatorial Atlantic; 3) finally, the relatively warm south equatorial waters are conducive to enhanced moisture and instability of the boundary layer flow. During the long dry season in northern Northeast Brazil, all of these general circulation features are near their opposite extreme, thus collectively hampering the precicpitation activity.

Subsaharan Africa (SAHEL in Fig. 1) has its rainy season at the height of the northern summer, when the near-equatorial confluence axis and associated convergence band reaches its northernmost position and the moist cross-equatorial monsoon flow penetrates deep into the interior of the continent (Lamb, 1978a,b, 1983; Hastenrath and Lamb, 1977a,b, 1978b). During the long dry season, the confluence axis and convergence band lie far to the south and dry desert air dominates the Sahel.

The rainy season on the Angola coast (ANGOLA in Fig. 1) is narrowly concentrated in March–April, when the surface waters of the eastern South Atlantic are warmest, thus favoring the instability and moisture of the boundary-layer flow into the continent (Hirst and Hastenrath, 1983a).

Concerning the annual cycle characteristics of circulation and rainfall in the Zaïre and Amazon basins and at the Ecuador–Peru coast (ZAIRE, AMAZON and EC/PERU in Fig. 1), refer to Hirst and Hastenrath (1983b), Ratisbona (1976) and Wyrtki (1975). The latter three regions are of subordinate interest in the following sections.

4. Regional rainfall anomalies and interannual variability of circulation

This section draws on the earlier series of regional studies to present the general circulation diagnostics of hydrometeorological anomalies in key land areas adjacent to the tropical Atlantic Ocean. In order to facilitate the comparison of interannual circulation and climate variability with the prominent characteristics of the annual march as summarized in Figs. 2a–f, a corresponding analysis mode is chosen in the anomaly maps (Figs. 3, 4, 5, 7) which are consistent with the various earlier diagnostic studies (Hastenrath, 1976, 1978; Hastenrath and Heller, 1977; Markham and McLain, 1977; Covey and Hastenrath, 1978; Lamb, 1978a,b; Moura and Shukla, 1981; Chu, 1983; Hirst and Hastenrath, 1983a,b) The maps Figs. 3, 4, 5 and 7 of indicative atmospheric and hydrospheric fields display composites of extremely WET minus extremely DRY years, for the important times of year, in selected land areas.

The collectives of WET and DRY years are identified from long-term hydrometeorological series. Reference is made to the various aforementioned regional studies for details and only a brief description is given here. Index series of hydrometeorological conditions are constructed, in most instances, from large ensembles of rainfall stations but also from observations of river level, so as to safeguard against the notorious temporal and spatial variability of tropical rainfall. Compilations are, as a rule, by 12 month intervals or entire rainy seasons. From such index series, the most extreme wet and dry years are identified and atmospheric and oceanic fields are analyzed for composites of such extreme years. The number of years used in the various regional studies ranges between 10 and 5 (refer to captions of Figs. 3, 4, 5, 7). Insistence on an identical number of years for all regions would require the inclusion of less extreme years and is not meaningful.

The reality of departure patterns is to be ascertained from the internal consistency between the various atmospheric and oceanic fields. In addition, the aforementioned regional studies used various independent and mutually supportive methods, such as stratification, spatial correlation and principal component analysis. Moreover, application of the two-tailed t-test as described in DeGroot (1975, 429–432, 580–581) is briefly summarized here.

For individual 5 degree blocks and various elements, the difference of the mean of a composite of extreme WET years and the mean of a composite of extreme DRY years (each 10 years or less; see captions of Figs. 3, 4, 5 and 7) is to be tested. The t-test is based on the premise that the two collectives are i) random samples, and ii) normally distributed and iii) have common variance (DeGroot, 1975, 429–432; Chu, 1983). Divergence is excluded from testing because, being a derived field and thus vulnerable to noise, it can only be computed from the composite mean surface wind rather than for individual years. The likelihood ratio test (DeGroot, 1975, 429–432) and 5 and 10 percent significance levels are used. For positive (negative) WET departures, the hypothesis to be tested is that the mean of the WET composite is significantly larger (smaller) than the mean of the DRY composite. Areas in which the 5 and 10 percent significance levels are reached are identified in Figs. 3, 4, 5, and 7. While statistically one twentieth (one tenth) of the area is expected to reach the 5 (10) percent significance level by chance, only a limited portion of the map area for a given field is highly relevant meteorologically. Accordingly, in the interpretation of t-test results, attention is to be focused on such relevant areas or elements. In fact, the consideration of the various atmospheric and oceanic fields in the context of the large-scale circulation provides an *a priori* hypothesis for the assessment of statistical field significance, as referred to by Livezey and Chen (1983). Their recent paper offers a novel and more appropriate approach to the statistical significance testing of departure patterns.

For the Central American–Caribbean region, the general circulation diagnostics of rainfall anomalies are illustrated by Figs. 3a–f. An abundant rainy season is associated with anomalously low pressure on the equatorward side of the North Atlantic high (Fig. 3a), a poleward displacement of the North Atlantic trades (Fig. 3b), anomalously warm North Atlantic waters in a band between about 10 and 20°N extending from the African coast all the way to the Americas (Fig. 3d) and enhanced convergence (Fig. 3e) and cloudiness (Fig. 3f) over the Caribbean and the adjacent low-latitude Atlantic. For a deficient rainy season, a sign convention broadly inverse to abundant rainfall years would apply. The t-test shows statistical significance at the chosen levels in the core areas of the prominent positive and negative zonal wind departures in the North Atlantic (Fig. 3b), in the band of positive SST departures across the North Atlantic (Fig. 3d) and less markedly in the realm of negative SLP departures in the North Atlantic (Fig. 3a).

The essential departure features of the SLP, wind, convergence and cloudiness fields appear internally consistent and related to decreased pressure on the equatorward side of the North Atlantic subtropical high. The SST departures are prominent, but their origin is not yet understood—as is the case for climate anomalies in many tropical regions. The statistical test supports the essential features in the meteorologically relevant areas of the zonal wind and SST fields, and to a lesser extent the SLP pattern, but not the enhanced cloudiness. Concerning the SST map (Fig. 3d), statistical significance is reached in a substantial portion of the band of positive departures in the North Atlantic.

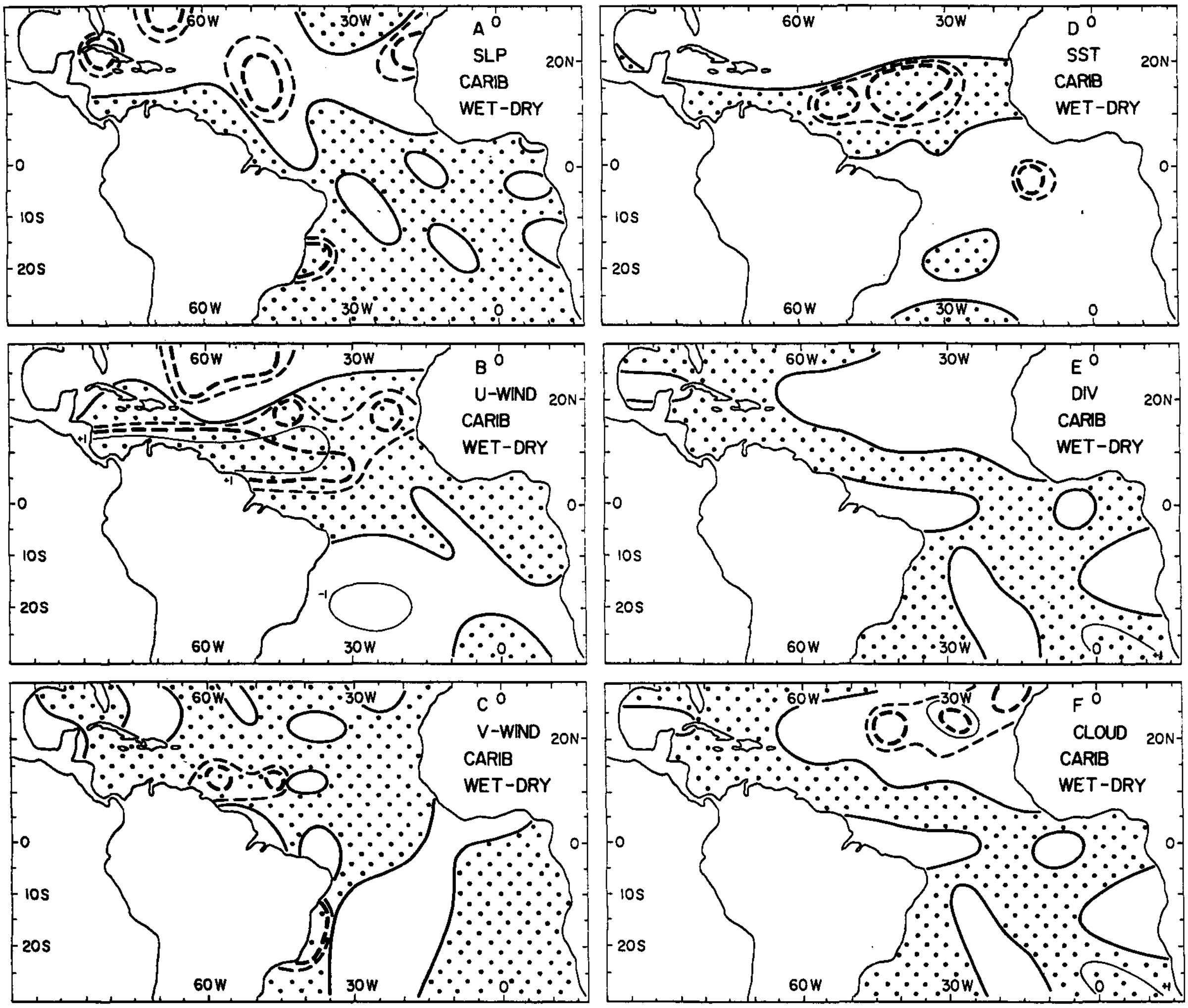

FIG. 3. Maps of July–August circulation departures associated with rainfall anomalies in the Central American–Caribbean region. Charts represent the difference of departures for the composite of WET years (1924, 27, 32, 33, 36, 38, 54, 56, 60, 66) minus the departures for the composite of DRY years (1925, 30, 39, 40, 46, 47, 57, 59, 65 and 72). (a)–(f) as in Fig. 2. Areas significant at the 5 and 10% levels are enclosed, respectively, by heavy and thin broken lines, (e) being excepted from testing.

Data are sparse in much of the realm of negative departures in the South and equatorial Atlantic and statistical significance is indicated only in a very limited area. Figs. 3a–f which illustrate the diagnostics of interannual circulation and climate variability, resemble in the most essential features the annual cycle of circulation patterns in the Atlantic domain as summarized in Figs. 2a–f. The same factors described in Section 3 as annual cycle mechanisms producing the alternation of dry and rainy seasons in the Central American–Caribbean region appear operative in the interannual variability. In this perspective, the interannual variations of circulation and rainfall appear as enhancements and reductions of the annual cycle.

Figs. 4a–f present the circulation departure patterns associated with rainfall anomalies in the northern Nordeste of Brazil. The circulation departures typical of an abundant rainy season are as follows: the near-equatorial trough of low pressure is displaced southward (Fig. 4a), as is the confluence between the Northern and Southern Hemispheric trade wind airstreams (Figs. 4b, c) and the associated band of maximum convergence and cloudiness (Figs. 4e, f); surface waters of the equatorial and South Atlantic are anomalously warm, while negative SST departures prevail in much of the tropical North Atlantic (Fig. 4d). During drought years in Northeast Brazil, the departure patterns of the various atmospheric and oceanic fields are approximately inverse to those in wet years. The t-test shows statistical significance in the areas of positive (negative) SLP departures in the North (South) Atlantic (Fig. 4a), in the zonal wind field over the equatorial region (Fig. 4b), in the meridional wind field over the equatorial zone and the adjacent North Atlantic (Fig. 4c), in the

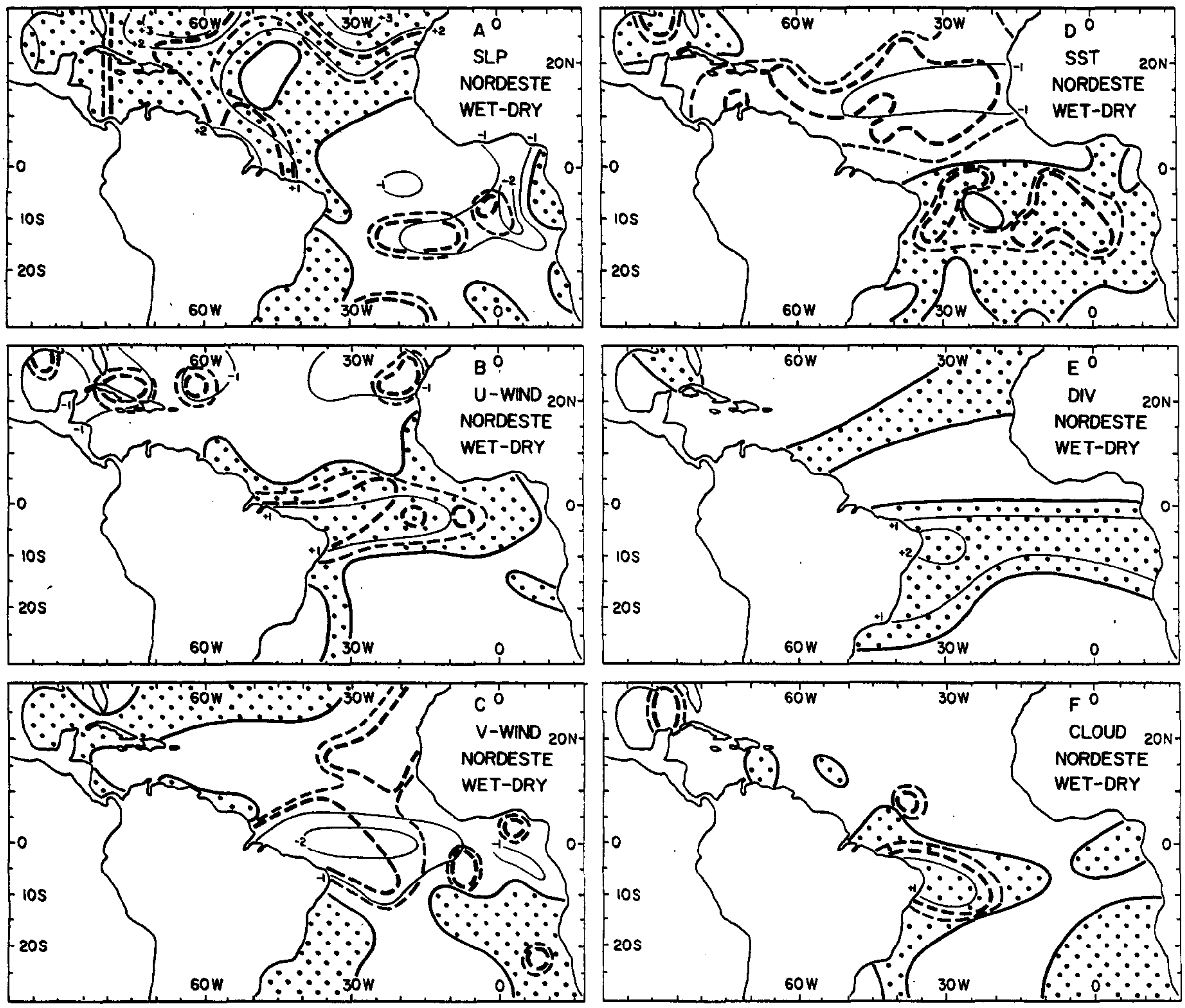

FIG. 4. Maps of March–April circulation departures associated with rainfall anomalies in the northern Nordeste of Brazil. The composite of WET years consists of 1917, 21, 22, 24, 26, 34, 35, 40, 64, 67 and the composite of DRY years of 1915, 19, 30, 32, 36, 42, 51, 53, 58. The meaning of charts is as in Fig. 3.

area of positive cloud departure over the equatorial Atlantic adjacent to Northeast Brazil (Fig. 4f) and in the core regions of negative (positive) SST departures in the low-latitude North (South) Atlantic (Fig. 4d). With regard to the SLP map (Fig. 4a), the large areas of statistical significance in the domain of positive departures in the North Atlantic are of particular interest. In the region of negative departures in the South Atlantic, where data coverage is less satisfactory, the area with statistical significance is more limited.

The departure characteristics of the pressure, wind and convergence fields are internally consistent and symptomatic of an anomalous latitude position of the near-equatorial trough. The band of anomalous convergence (Fig. 4c) extending from Brazil to equatorial Africa is matched by a corresponding zone of enhanced cloudiness (Fig. 4f). Our early results concerning the wind field have been duplicated by another analyst and the substantive features of the SST departure pattern have been duplicated by three other research groups (review in Hastenrath, 1983). However, the origin of the SST departures has remained enigmatic. The statistical test supports the essential features in the meteorologically relevant areas of the SLP, wind, SST and cloudiness fields. Again, the combination of general circulation factors favoring rainfall activity resembles those discussed in Section 3 for the annual cycle.

The circulation departure patterns characteristic of rainfall anomalies in Subsaharan Africa are presented in Figs. 5a–f. For an abundant rainy season, the following features are apparent over the eastern tropical Atlantic adjacent to West Africa. The near-equatorial trough of low pressure (Fig. 5a), the associated confluence between the Northern and Southern Hemispheric trade wind airstreams (Figs. 5b, c) and the

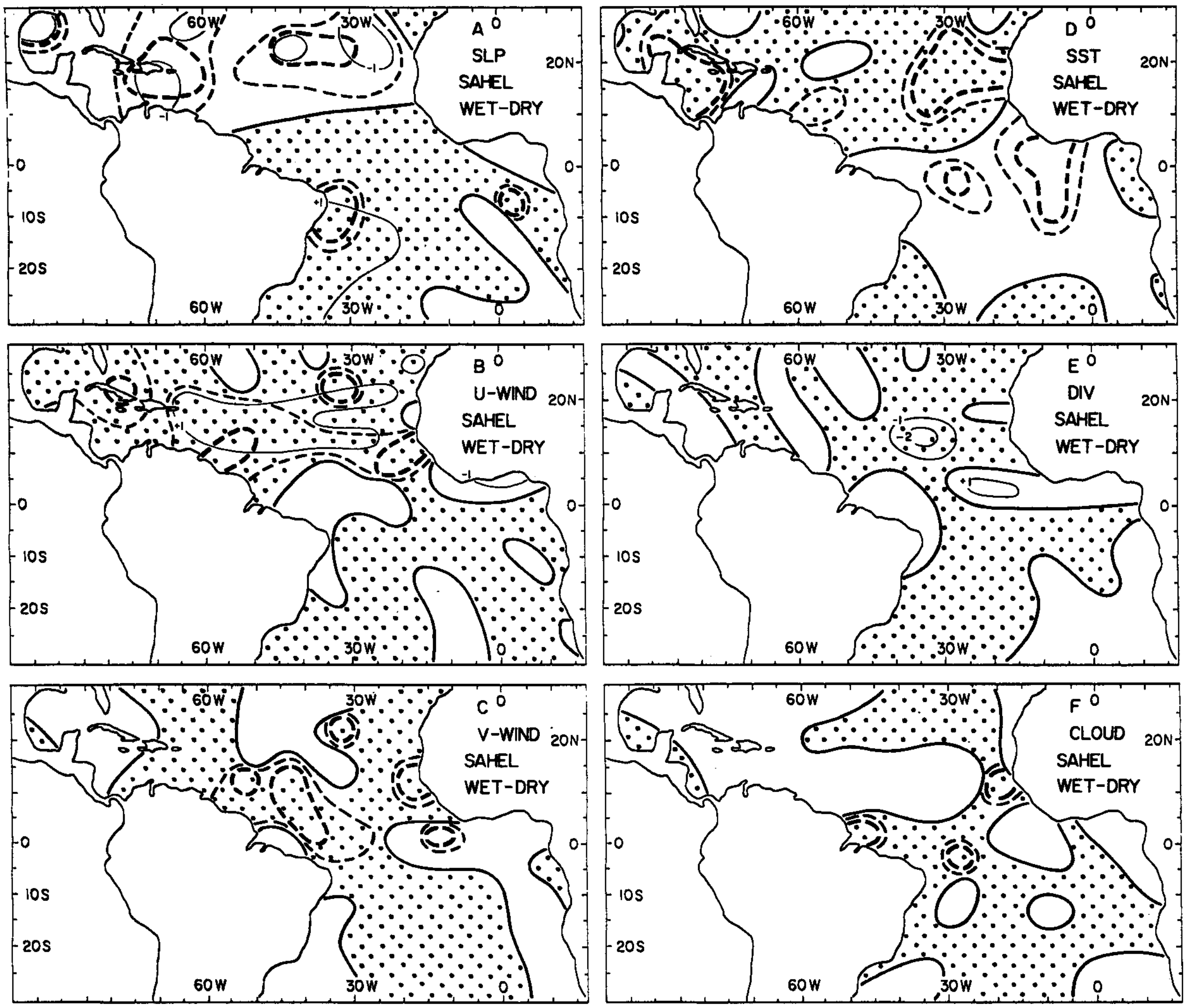

FIG. 5. Maps of July–August circulation departures associated with rainfall anomalies in Subsaharan Africa. The composite of WET years consists of 1943, 50, 52, 54, 55 and 57 and the composite of DRY years of 1941, 42, 44, 68, 70, 71 and 72. The meaning of charts is as in Fig. 3.

band of maximum convergence (Fig. 5e) are displaced northward, and the surface waters of much of the tropical North Atlantic are comparatively warm (Fig. 5d). Drought in Subsaharan Africa is associated with circulation departure patterns broadly inverse to those found in wet years. The t-test shows statistical significance in the realm of positive SST departure (Fig. 5d) and in the negative SLP area (Fig. 5a) in the North Atlantic.

The departures in the pressure and wind fields are internally consistent in indicating a northward displacement of quasi-permanent circulation features over the tropical Atlantic. SST departures are prominent, but their origin is not yet understood. The substantive departure features first pointed out by Lamb (1978a,b) were later duplicated by another analyst (review in Lamb, 1982). The statistical test supports the prominent characteristics of the SST maps (Fig. 5d), but only to a limited extent the other internally consistent fields. In brief, the general circulation mechanisms of interannual rainfall variability illustrated by Fig. 5 appear as discussed in Section 3 for the annual cycle.

The map of divergence, Fig. 5e, is complemented by the meridional profiles, Fig. 6. During the northern summer rainy season, the convergence band assumes a far poleward position and a zone of distinct divergence is found between the equator and about 5°N, while in the winter dry season, the convergence band is displaced southward under elimination of the near-equatorial divergence belt. In similarity to these annual cycle characteristics, the profile for the extreme drought year 1968 is characterized by a comparatively far equatorward position of the convergence band, while the moderately wet year 1967 features a poleward location of the convergence band along with a well-developed near-equatorial divergence zone. The com-

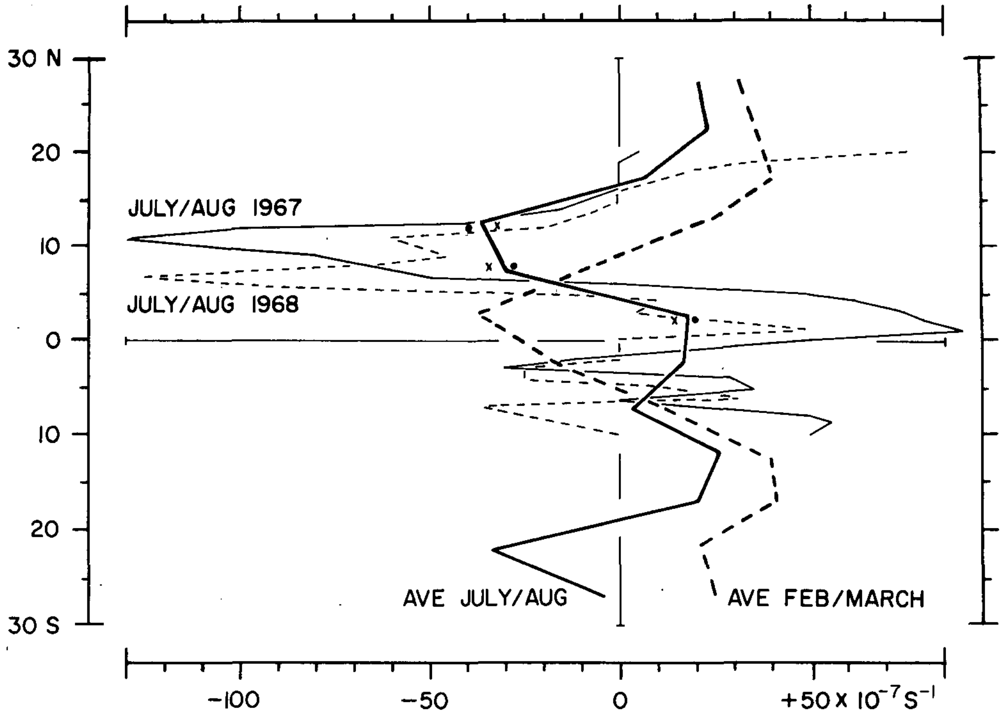

FIG. 6. Meridional profiles of divergence (10^{-7} s^{-1}) in the strip 10–30°W. The 60-year means of July–August and February–March are shown as heavy solid and broken lines respectively. Thin solid lines refer to the abundant rainfall year 1967, and thin broken lines to the extreme drought year 1968. In the latitude bands 0–5, 5–10 and 10–15°N, the values for the composites of six WET years and of seven DRY years are denoted by dots and crosses respectively.

posites of DRY and WET years depart from the 60-year mean July–August profile in the same sense as just described for the individual extreme years 1968 (dry) and 1967 (wet), but with much smaller amplitude. The features for the latter two profiles are more conspicuous in part because they are drawn with a one degree latitude resolution, whereas values for five degree strips are plotted for the DRY and WET composites and the 60-year average. Divergence is excluded from statistical significance testing for reasons explained above. Complementing Fig. 5, the meridional profiles in Fig. 6 illustrate that the divergence departures during dry (wet) years appear as reductions (enhancements) of the average annual cycle.

Figures 7a–f and Fig. 8 describe the circulation departure patterns associated with sea temperature and rainfall anomalies at the Angola coast. The maps in Fig. 7 are presented for conformity with the three regions previously discussed, but the more pertinent evidence is contained in Fig. 8. The following chain of causality is suggested (Hirst and Hastenrath, 1983a): the seasonal *relaxation* of wind stress over the western equatorial Atlantic from approximately November to March is associated with a warming of the eastern equatorial and South Atlantic surface waters; the high SST makes for increased moisture and instability of the lower-tropospheric flow into the continent. The latter contribute to increased rainfall activity at both the Angola coast and in the Zaïre basin. The seasonal *relaxation* of wind stress over the western equatorial Pacific, rather than the wind stress itself, is considered instrumental in this climate anomaly mechanism. Accordingly, the state of atmospheric and oceanic fields in a given season is less informative than the annual cycle evolution. In fact, most chart features in Fig. 7 do not satisfy the particular statistical test used in this paper. For Fig. 8a, the two-tailed t-test was applied to the difference between the WET and DRY values of seasonal wind stress relaxation (westward wind stress of September–October–November minus that of February–March–April), but results were not found significant at the 10 percent level. Fig. 8 illustrates that the aforementioned causality chain seems operative in the interannual variability of rainfall, which appears to result from enhancements and reductions of the annual cycle.

As a complement to these analyses (Figs. 3–8), three regions are considered where annual cycle characteristics do not seem to play a prominent role in the interannual variability of circulation and climate. Rainfall over the Zaïre basin and in Amazonia appear to be modulated by variations in a zonal circulation

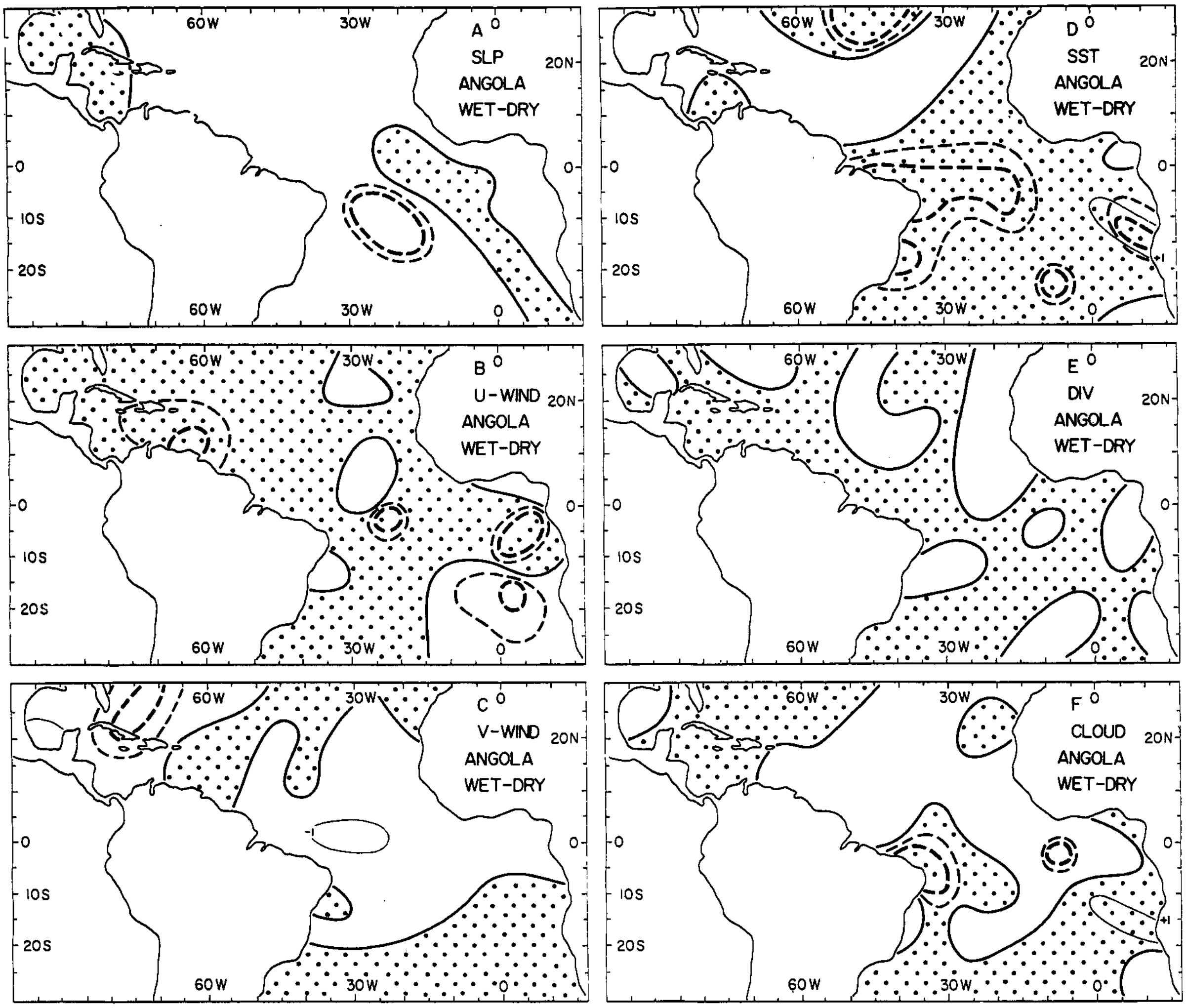

FIG. 7. Maps of March–April circulation departures associated with rainfall anomalies at the Angola coast. The composite of WET years consists of 1956/57, 62, 63, 69 and 71 and the composite of DRY years of 1952/53, 54, 58, 64 and 72. The meaning of charts is as in Fig. 3.

cell along the Atlantic equator. Concerning the El Niño events on the west coast of South America, an intertwining of annual and interannual variations similar to the Angola coast appears plausible (see also Wyrtki, 1975). Aside from the latter three regions, these diagnostic studies indicate that enhancements and reductions of the "normal" annual cycle may constitute the major general circulation mechanisms for the interannual variability of rainfall in key regions of the tropical Americas and Africa.

5. Summary and conclusions

A synopsis of various circum-Atlantic studies indicates that the interannual variability of climate and circulation bears a fairly close relationship to the annual cycle. The following conclusions are suggested by the evidence assembled in this paper, although not all of them are supported by conventional statistical significance testing.

For the Central American–Caribbean region, abundant rainfall at the height of the northern summer tends to be accompanied by low pressure on the equatorward side of the North Atlantic high and related features in the wind, cloudiness and SST fields. Increased convergence, along with the SST-induced enhancement of atmospheric moisture and instability, favors precipitation.

Abundant rainfall in northern Northeast Brazil around March–April is associated with a far southerly position of the near-equatorial low-pressure trough and concomitant confluence, convergence and cloudiness bands and relatively cold waters in the North Atlantic and positive SST anomalies in the equatorial and South

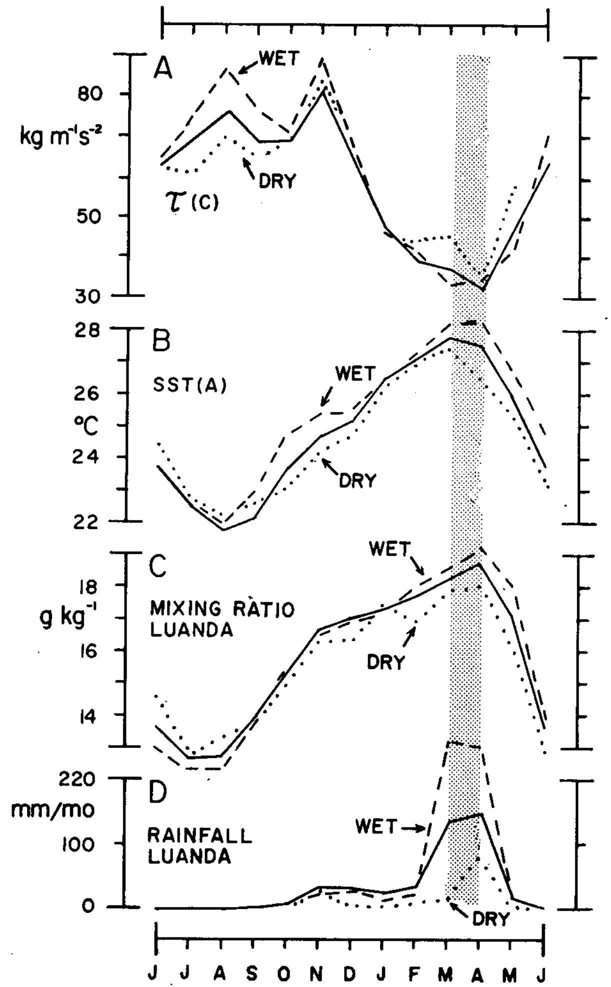

FIG. 8. Annual march of (a) westward wind stress over the western equatorial Atlantic (5°N–5°S, 10–40°W), (b) SST off southwestern Africa (0–10°S, 0–15°E, and 10–15°S, 5–15°E), (c) surface mixing ratio at Luanda–Angola, (d) rainfall at Luanda. Solid, broken and dotted lines refer to the 1948–72 average, and the WET and DRY composites (years given in caption of Fig. 7) respectively, from Hirst and Hastenrath (1983a).

Atlantic. This configuration is conducive to rainfall through at least three cooperative mechanisms.

Subsaharan Africa generally receives its most abundant rainfall at the height of the northern summer with a far northerly position of the near-equatorial low-pressure trough and associated features in the wind, cloudiness and SST fields.

The March–April rainfall at the Angola coast has antecedents of remote forcing. A relaxation of easterly wind stress over the western equatorial Atlantic from approximately November to March is associated with warm surface waters in the eastern South Atlantic, which in turn have thermodynamic consequences for the atmospheric boundary layer flow.

All of the aforementioned causality chains affecting the rainfall activity appear operative both as part of the annual cycle and as general circulation mechanisms of interannual variability. Processes not obviously related to the annual cycle seem to play a role in the interannual variability of rainfall in the Amazon and Zaïre basins. However, this study suggests that much of the interannual variability in the climate of certain key regions of the tropical Atlantic sector results from enhancement and reduction of the annual cycle. In this perspective, it should be realized that the general circulation mechanisms pertaining to the annual cycle are at present hardly better understood than the interannual variability of climate and circulation.

Acknowledgment. This study was supported by NSF Grant ATM82-00511.

REFERENCES

Chu, P. S., 1983: Diagnostic studies of rainfall anomalies in Northeast Brazil. *Mon. Wea. Rev.*, **111**, 1655–1664.

——, and S. Hastenrath, 1982: *Atlas of Upper-Air Circulation over Tropical South America.* Department of Meteorology, University of Wisconsin, Madison, WI 53706, 237 pp.

Covey, D. C., and S. Hastenrath, 1978: The Pacific El Niño phenomenon and the Atlantic circulation. *Mon. Wea. Rev.*, **106**, 1280–1287.

DeGroot, M. H., 1975: *Probability and Statistics.* Addison-Wesley, 607 pp.

Environmental Science Service Administration, 1967: *World Weather Records 1951–1960,* Vols. 3 and 5: *South America and Africa.* U.S. Government Printing Office, Washington, DC 20550, 355 and 574 pp.

Hastenrath, S., 1966: On general circulation and energy budget in the area of the Central American Seas. *J. Atmos. Sci.*, **23,** 694–711.

——, 1967: Rainfall distribution and regime in Central America. *Arch. Meteor. Geophys. Bioklim.*, **B15,** 201–241.

——, 1976: Variations in low-latitude circulation and extreme climatic events in the tropical Americas. *J. Atmos. Sci.*, **33,** 202–215.

——, 1978: On modes of tropical circulation and climate anomalies. *J. Atmos. Sci.*, **35,** 2222–2231.

——, 1983: Comments on "Correlation between the tropical Atlantic trade winds and precipitation in Northeastern Brazil". *J. Climatol.*, **3,** 207–209.

——, and L. Heller, 1977: Dynamics of climatic hazards in Northeast Brazil. *Quart. J. Roy. Meteor. Soc.*, **103,** 77–92.

——, and P. J. Lamb, 1977a: *Climatic Atlas of the Tropical Atlantic and Eastern Pacific Oceans.* The University of Wisconsisn Press, Madison, WI 53706, 113 pp.

——, and ——, 1977b: Some aspects of circulation and climate over the eastern equatorial Atlantic. *Mon. Wea. Rev.*, **106,** 1280–1287.

——, and ——, 1978a: *Heat Budget Atlas of the Tropical Atlantic and Eastern Pacific Oceans.* University of Wisconsin Press, Madison, WI 53706, 103 pp.

——, and ——, 1978b: On the dynamics and climatology of surface flow over the equatorial oceans. *Tellus,* **30,** 436–448.

Hirst, A. C., and S. Hastenrath, 1983a: Atmosphere–ocean mechanisms of climate anomalies in the Angola–tropical Atlantic sector. *J. Phys. Oceanogr.*, **13,** 1146–1157.

——, and ——, 1983b: Diagnostics of hydrometeorological anomalies in the Zaïre (Congo) basin. *Quart. J. Roy. Meteor. Soc.*, **109**, 879–890.

Jackson, S. P., 1964: *Climatic Atlas of Africa.* Government Printer, Pretoria, South Africa, 117 pp.

Lamb, P., 1978a: Case studies of tropical Atlantic surface circulation pattern during recent Sub-Saharan weather anomalies: 1967 and 1968. *Mon. Wea. Rev.*, **106**, 482–491.

——, 1978b: Large-scale tropical Atlantic circulation patterns associated with Subsaharan weather anomalies. *Tellus,* **30**, 240–251.

——, 1982: Comments on "West African rainfall variations and tropical Atlantic sea surface temperatures". *Climate Monitor,* **11**, 46–49.

——, 1983: West African water vapor variations between recent contrasting Subsaharan rainy seasons. *Tellus,* **35A**, 198–212.

Livezey, R. E., and W. Y. Chen, 1983: Statistical field significance and its determination by Monte Carlo techniques. *Mon. Wea. Rev.*, **111**, 46–59.

Markham, C. G., and D. R. McLain, 1977: Sea surface temperature related to rain in Ceara, Northeast Brazil. *Nature,* **265**, 320–323.

Moura, A. D., and J. Shukla, 1981: On the dynamics of droughts in Northeast Brazil: Observations, theory, and numerical experiments with a general circulation model. *J. Atmos. Sci.*, **38**, 2653–2675.

Ratisbona, L. R., 1976: The climate of Brazil. *World Survey of Climatology,* Vol. 12, Elsevier, 219–269.

Sadler, J. C., 1975: The upper-tropospheric circulation over the global tropics. Department of Meteorology, University of Hawaii, Honolulu, HI 96822, UHMET-75-05, 35 pp.

Smithsonian Institution, 1927, 1934, 1947: *World Weather Records (*up to *1920, 1921–30, 1931–40).* Smithsonian Miscellaneous Collections, Vols. 79, 90, 105, Washington, DC 20550; 1199, 616, 646 pp.

Taljaard, J. J., H. van Loon, H. L. Crutcher and R. L. Jenne, 1969: *Climate of the Upper Air: Southern Hemisphere.* Vol. 1, *Temperatures, Dew Points and Heights at Selected Pressure Levels.* NAVAIR 50-1C-55, Chief Naval Operations, Washington, DC 20550, 135 pp.

Thompson, B. W., 1965: *The Climate of Africa.* Oxford University Press, 132 pp.

U.S. Weather Bureau, 1959: *World Weather Records 1941–50.* U.S. Government Printing Office, Washington, DC 20550, 574 pp.

——, ESSA, NOAA, 1958–1981: *Monthly Climatic Data for the World,* Vols. 11–34. National Climatic Center, Asheville, NC 28801.

Wyrtki, K., 1975: El Niño—the dynamic response of the Equatorial Pacific Ocean to atmospheric forcing. *J. Phys. Oceanogr.*, **5**, 572–584.